AIAA JOURNAL
Vol. 40, No. 5, May 2002

Aeroelastic Response and Flutter of Swept Aircraft Wings

Piergiovanni Marzocca* and Liviu Librescu†
Virginia Polytechnic Institute and State University, Blacksburg, Virginia 24061-0219
and
Walter A. Silva‡
NASA Langley Research Center, Hampton, Virginia 23681-2199

A unified approach of stability and aeroelastic response of swept aircraft wings in an incompressible flow is developed. To this end, the indicial function concept in time and frequency domains is used, and on this basis the flutter instability and subcritical aeroelastic response to arbitrary time-dependent external excitation are analyzed. In addition, an original representation of the aeroelastic response in the phase space is presented, and the implications of the related results toward determining the flutter instability in flight are emphasized. Validations of selected results against the theoretical and experimental predictions are supplied, and pertinent conclusions are outlined.

Nomenclature

a_n	=	dimensionless elastic axis position measured from the midchord, positive aft
$C(k)$, $F(k)$, $G(k)$	=	Theodorsen's function and its real and imaginary parts, respectively
$C_{L\alpha_n}$	=	local lift-curve slope for a section normal to the elastic axis in steady flow
c_n	=	chord length of wing, normal to the elastic axis, $2b_n$
f_h, f_α	=	plunging and pitching decoupled eigenmodes, respectively
H_i, A_i	=	dimensionless unsteady aerodynamic coefficients
h, h_0, ξ	=	plunging displacement, its amplitude, and dimensionless counterpart, h/b_n, respectively
I_y, $\bar{r}_\alpha$	=	mass moment of inertia per unit span wing and the dimensionless radius of gyration, $(I_y/mb_n^2)^{1/2}$, respectively
i	=	imaginary unit, $\sqrt{-1}$
L_i, M_i	=	dimensionless unsteady aerodynamic complex coefficients
${}_\Lambda L_a$, ${}_\Lambda M_a$	=	total lift and moment about the elastic axis per unit span of the swept wing
L_b, l_b	=	overpressure due to an N-wave shock pulse and its dimensionless counterpart, $L_b b_n/mU_n^2$, respectively
$\mathcal{L}$, s	=	Laplace operator and Laplace variable, respectively
l	=	wing semispan measured along the midchord line
l_a, m_a	=	dimensionless aerodynamic lift, $L_a b_n/mU_n^2$, and moment, $M_a b_n^2/I_y U_n^2$, respectively
m, μ	=	wing mass per unit length and wing/air mass ratio, $m/\pi\rho b_n^2$, respectively
N	=	load factor, $1 + h''/g$
P_m, $\wp_m$	=	peak reflected pressure in excess of the ambient one and its dimensionless counterpart $P_m b_n/mU_n^2$, respectively
r	=	shock pulse length factor
S_α, $\bar{\chi}_\alpha$	=	static unbalance about the elastic axis and its dimensionless counterpart, S_y/mb_n, respectively
t	=	time variable
U_∞, U_n, V_n	=	freestream speed, its component normal to the elastic axis, and the dimensionless counterpart, $U_n/b_n\omega_\alpha$, respectively
w	=	downwash velocity
x, y	=	coordinates parallel and perpendicular to freestream direction
$\bar{x}$, $\bar{y}$	=	chordwise (normal to the elastic axis) and spanwise (along the elastic axis) coordinates
z, Z	=	transverse normal coordinate to the midplane of the wing and the vertical displacement in z direction, respectively
α, α_0	=	twist angle about the elastic axis and its amplitude, respectively
δ_r	=	tracer quantity
ζ_h, ζ_α	=	structural damping ratio in plunging, $c_h/2m\omega_h$, and in pitching, $c_\alpha/2I_y\omega_\alpha$, respectively
η	=	dimensionless coordinate along the wing span, $\bar{y}/l$
Λ	=	sweep angle (positive for swept back)
λ, σ	=	spanwise rate of change of twist and bending, respectively
ρ	=	air density
τ	=	dimensionless time, $U_n t/b_n$
τ_p	=	dimensionless positive phase duration of the pulse, measured from the time of the arrival
τ_w	=	parameter identifying the propagation speed of the gust V_g with respect to V_n
$\phi(\tau)$, $\Phi(s)$	=	Wagner's function in time and Laplace domains, respectively
ω, k_n	=	circular and reduced frequencies, $\omega b_n/U_n$, respectively
$\bar{\omega}$	=	plunging–pitching frequency ratio, ω_h/ω_α
ω_h, ω_α	=	uncoupled frequency in plunging, $(K_h/m)^{1/2}$, and pitching, $(K_\alpha/I_y)^{1/2}$, respectively

Subscripts

c, nc	=	circulatory and noncirculatory terms of lift and aerodynamic moment, respectively
n	=	quantity normal to the elastic axis
Λ	=	quantity associated with the swept wing

Received 26 May 2000; revision received 9 July 2001; accepted for publication 29 October 2001.

*Visiting Assistant Professor, Department of Engineering Science and Mechanics, 0219 Norris Hall. Member AIAA.
†Professor of Aeronautical and Mechanical Engineering, Department of Engineering Science and Mechanics, 0219 Norris Hall; librescu@vt.edu.
‡Senior Research Scientist and Senior Aerospace Engineer, Aeroelasticity Branch, Structures and Materials Competency. Senior Member AIAA.

Superscripts

$\hat{\ }$ = variables in Laplace transformed space
$\cdot, '$ = derivatives with respect to the time t and the dimensionless time τ, respectively

I. Introduction

In this paper, the concept of indicial[1–3] functions in time and frequency domains is used to determine, for incompressible flowfields, the associated unsteady aerodynamic derivatives for swept lifting surfaces. Such a treatment of the problem enables one to approach, in a unified way, both the aeroelastic response in the subcritical flight speed regime to arbitrary time-dependent external excitations (such as explosive airblasts and sonic boom[4,5]) and the flutter instability of swept wings. In this paper, both problems are addressed.

As a byproduct of this analysis, a closed-form solution of unsteady aerodynamic derivatives, including corrections for aspect ratio, sweep angle, and camber effect, is obtained. This modified version can easily be implemented and used in aeroelastic response problems including flutter analyses.

The unsteady aerodynamic lift and moment in the incompressible flight speed regime are expressed for the swept aircraft wing in the time and frequency domains by the use of Wagner's and Theodorsen's functions, respectively. For aeroelastic response, it is only necessary to express the lift and moment via the indicial Wagner's function. Toward the approach of the flutter problem, two avenues have been pursued here, namely, that based on complex eigenvalue analysis and on aeroelastic response. Whereas Theodorsen's function helps with the conversion of the expressions of both the aerodynamic loads and of unsteady aerodynamic derivatives in the frequency domain, their Laplace domain counterparts are directly applicable in aeroelastic response problems.[6,7]

Within this unified approach, the flutter instability from the data related to the aeroelastic response will be evaluated.

Herein, a swept aircraft wing (Figs. 1 and 2) that features the plunging h and pitching α degrees of freedom and that is exposed to a two-dimensional incompressible flow is used. The concept of swept wing generated by rotation was adopted (Fig. 1), and the wing structure is modeled within the Bernoulli–Euler hypothesis.

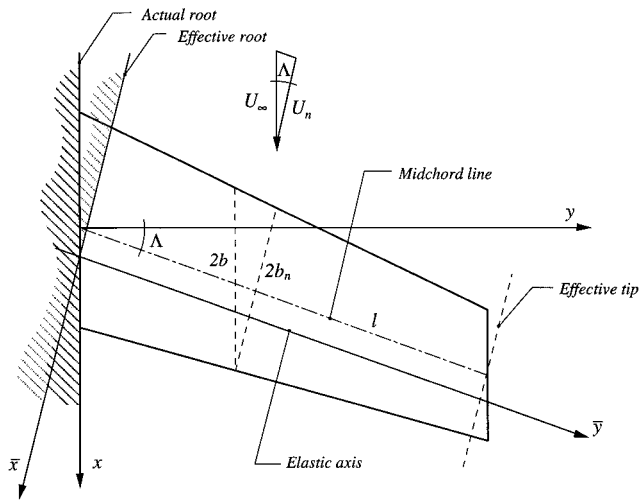

Fig. 1 Nonuniform swept wing.

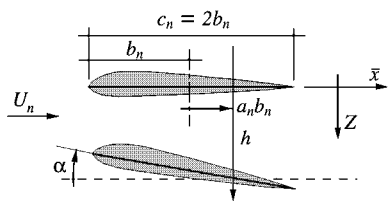

Fig. 2 Airfoil section.

As a basic assumption, the oscillatory motion is represented as a combination of the uncoupled bending and twisting vibrating modes of the wing.

In connection with the various loads intervening in the aeroelastic governing equations, the distinction between unsteady aerodynamic and gust loads, on one hand, and blast loads, on the other hand, was clearly described by Bisplinghoff et al.,[1] and this point of view was adopted in this paper as well.

The results of this approach are valid if the blast pulses are characterized by small to moderate loading intensities. As a result, although these are not able to cause severe damage, the induced vibration can lead to failure by fatigue of the structure. For most problems of this nature, these conditions are likely to be satisfied unless the wing structure is far away from the center of the blast/sonic boom. As was clearly stated in Ref. 8, the limiting distance depends on the magnitude of the blast, the orientation relative to the wing structure, the speed of the aircraft, and the geometry of the wing.

As was shown by Yates,[9] the use of modified strip theory aerodynamics provides very good results for moderate to large aspect ratio wings and for moderate sweep angles, up to $\Lambda = 60$ deg. Within the present aerodynamic modeling, the corrections involving the lift-curve slope (which are related to the sweep angle and aspect ratio), are extracted from the steady aerodynamics of flat rigid wings. Moreover, in contrast to the usual procedure of discarding the camber deformation of sections normal to the elastic axis, this effect, which becomes prominent for small-aspect-ratio wings, has been taken into account.

Because in the present work a uniform swept wing in an incompressible flowfield is considered, Yates's modified two-dimensional strip theory involves, as the improvement, only the expression of the three-dimensional section lift-curve slope. The aerodynamic center is located at the quarter chord on each cross section of the wing.

Although here a fixed lift-curve slope in the spanwise direction was used, extension to a spanwise-varying lift-curve slope based on steady three-dimensional solutions for the wing is straightforward. The approach and results of aeroelastic response to gust and blast loads can be useful in the preliminary design and are likely to contribute to a better understanding of the implications of a number of parameters related to the wing geometry and the characteristics of the blast on the dynamic response of the wing. Moreover, extension of this methodology toward the unified nonlinear aeroelastic approach by using nonlinear aerodynamic indicial functions constitutes the next goal of this research.

II. Preliminaries

As shown in Ref. 10, for zero initial conditions, the unsteady aerodynamic loads can be converted from the time to the frequency domain via a Laplace transform. This results in the possibility of using the correspondence $s \to ik_n$ to convert the unsteady aerodynamic load from the time to the frequency domain, where s and k_n are the Laplace transform variable and the reduced frequency, respectively. The Laplace transform operator $\mathcal{L}$ is defined as

$$\mathcal{L}(\cdot) = \int_0^\infty (\cdot) e^{-s\tau}\, d\tau \tag{1}$$

whereas Wagner's function $\phi(\tau)$ is connected with Theodorsen's function $C(k_n)$, via a Laplace transform, as

$$C(k_n) = F(k_n) + iG(k_n) = ik_n \int_0^\infty \phi(\tau) e^{-ik_n\tau}\, d\tau = ik_n \Phi(ik_n) \tag{2}$$

and vice versa

$$\phi(\tau) = \mathcal{L}^{-1}\{C(k_n)/ik_n\}, \qquad Re(ik_n) > 0 \tag{3}$$

Using the correspondence $s \leftrightarrow ik_n$, we can also write

$$\Phi(ik_n)_{ik_n \to s} = \int_0^\infty \phi(\tau) e^{-s\tau}\, d\tau = \Phi(s) \tag{4}$$

Use of this relationship enables one to obtain the full expression of unsteady aerodynamic derivatives in terms of Theodorsen's

circulation function $C(k_n)$ and its real and imaginary components $F(k_n)$ and $G(k_n)$ in the frequency domain, or their counterpart in the Laplace domain, as well. Note that the reduced frequency parameter k_n for swept and straight wings coincide:

$$k_n = \frac{\omega b_n}{U_n} = \frac{\omega b \cos\Lambda}{U_\infty \cos\Lambda} = \frac{\omega b}{U_\infty} = k, \qquad i\omega t = i k_n \tau \tag{5}$$

This implies that the indicial Wagner's function $\phi(\tau)$ remains invariant to any change of the sweep angle.

III. Analytical Developments

For swept wings in an incompressible flowfield, the total lift per unit span can be expressed in a way similar to that reported for a two-dimensional airfoil by Fung[11]:

$${}_\Lambda L_a(\bar{y}, t) = {}_\Lambda L_c(\bar{y}, t) + {}_\Lambda L_{\mathrm{nc1}}(\bar{y}, t) + {}_\Lambda L_{\mathrm{nc2}}(\bar{y}, t) + {}_\Lambda L_{\mathrm{nc3}}(\bar{y}, t) \tag{6}$$

Herein, the indices c and nc identify the various contributions associated with the circulatory and noncirculatory terms, respectively. With similar notations, the total moment per unit span about the elastic axis is

$${}_\Lambda M_a(\bar{y}, t) = {}_\Lambda M_c(\bar{y}, t) + {}_\Lambda M_{\mathrm{nc1}}(\bar{y}, t) + {}_\Lambda M_{\mathrm{nc2}}(\bar{y}, t) + {}_\Lambda M_{\mathrm{nc3}}(\bar{y}, t) + {}_\Lambda M_{\mathrm{nca}}(\bar{y}, t) \tag{7}$$

${}_\Lambda M_{\mathrm{nca}}(\bar{y}, t)$ being associated with the apparent moment of inertia.[11] The lift is positive upward, whereas the moment is positive nose up. For the sake of convenience, the plunging coordinate is positive downward (see Fig. 2). When the vertical displacement Z of a point on the centerline of the cross section of the wing is expressed as[12]

$$Z(\bar{x}, \bar{y}, t) = h(\bar{y}, t) + \bar{x}\alpha(\bar{y}, t) \tag{8}$$

where $h \equiv h(\bar{y}, t)$ and $\alpha \equiv \alpha(\bar{y}, t)$ are the displacements in plunging and pitching, respectively, and one assumes that the origin of the $\bar{x}$ axis coincides with the elastic center, the downwash velocity w normal to the lifting surface becomes

$$w(x, y, t) \equiv w(\bar{x}, \bar{y}, t) = \frac{\partial Z}{\partial t} + U_\infty \frac{\partial Z}{\partial \bar{x}} \tag{9}$$

The in-plane chordwise coordinate $\bar{x}$ normal to the elastic axis (see Figs. 1 and 2) can be expressed as

$$\bar{x} = b_n\left(\tfrac{1}{2} - a_n\right) \tag{10}$$

Consequently, by use of the dimensionless time $\tau (\equiv U_n t/b_n)$, Eq. (9) becomes

$$w(\bar{x}, \bar{y}, \tau) = U_n\left[\frac{h'}{b_n} + \alpha + \frac{\partial h}{\partial \bar{y}}\tan\Lambda + \left(\frac{1}{2} - a_n\right)\left(\alpha' + \underline{b_n \frac{\partial \alpha}{\partial \bar{y}}\tan\Lambda}\right)\right] \tag{11}$$

where b_n is the half-chord of the airfoil, U_n is the component of the flow speed, both normal to the elastic axis, and $(\cdot)' \equiv \partial(\cdot)/\partial\tau$. The underlined quantity in Eq. (11) is related to the wing camber effect. Because its effect is rather small for high aspect ratio wings, it is usually discarded in the specialized literature.[1,13] However, herein, this effect will be taken into consideration.

In the following sections, the unsteady aerodynamic loads are obtained in the time domain (Sec. III.A.1) and via the use of the Laplace transform in the frequency domain (Sec. III.A.2). The unsteady aerodynamic derivatives are expressed in the frequency domain (Appendix A) and converted in the Laplace domain to be used toward the flutter evaluation.

A. Unsteady Aerodynamic Loads in Incompressible Flow

1. Time Domain

The circulatory component of the lift, expressed in terms of Wagner's indicial function $\phi(\tau)$ (referred also to as heredity function), obtained in the time domain, is[12]

$${}_\Lambda L_c(\bar{y}, \tau) = -C_{L\alpha_n} b_n \rho U_n^2 \int_{-\infty}^{\tau} \phi(\tau - \tau_0)\left[\frac{h''}{b_n} + \alpha' + \frac{\partial^2 h}{\partial \bar{y}\partial\tau_0}\tan\Lambda + \left(\frac{1}{2} - a_n\right)\left(\alpha'' + b_n \frac{\partial^2 \alpha}{\partial \bar{y}\partial\tau_0}\tan\Lambda\right)\right] \mathrm{d}\tau_0 \tag{12}$$

The aerodynamic noncirculatory components, using the dimensionless time, are expressed as

$${}_\Lambda L_{\mathrm{nc1}}(\bar{y}, \tau) = -\frac{1}{2} C_{L\alpha_n} \rho U_n^2 [h'' - a_n b_n \alpha''] \tag{13a}$$

$${}_\Lambda L_{\mathrm{nc2}}(\bar{y}, \tau) = -\frac{1}{2} C_{L\alpha_n} \rho U_n^2 b_n \alpha' \tag{13b}$$

$${}_\Lambda L_{\mathrm{nc3}}(\bar{y}, \tau) = -\frac{1}{2} C_{L\alpha_n} \rho U_n^2 b_n^2 \tan\Lambda\left[(\delta_r + 1)\frac{\sigma'}{b_n} + \delta_r \lambda + \delta_r \frac{\partial \sigma}{\partial \bar{y}}\tan\Lambda\right] + \frac{1}{2} a_n C_{L\alpha_n} \rho U_n^2 b_n^3 \tan\Lambda\left[(\delta_r + 1)\frac{\lambda'}{b_n} + \delta_r \frac{\partial \lambda}{\partial \bar{y}}\tan\Lambda\right] \tag{13c}$$

By the use of the expression of the lift [Eq. (6)], the equation for the moment [Eq. (7)] can be cast as

$${}_\Lambda M_a(\bar{y}, t) = -\left(\tfrac{1}{2} + a_n\right) b_n {}_\Lambda L_c(\bar{y}, t) - a_n b_n {}_\Lambda L_{\mathrm{nc1}}(\bar{y}, t) + \left(\tfrac{1}{2} - a_n\right) b_n {}_\Lambda L_{\mathrm{nc2}}(\bar{y}, t) + {}_\Lambda M_{\mathrm{nc3}}(\bar{y}, t) + {}_\Lambda M_{\mathrm{nc}}(\bar{y}, t) \tag{14}$$

in which, using the dimensionless time, the last two noncirculatory components are expressed as

$${}_\Lambda M_{\mathrm{nc3}}(\bar{y}, \tau) = -\frac{1}{2} C_{L\alpha_n} \rho U_n^2 b_n^3 \frac{1}{2}\lambda \tan\Lambda - a_n b_n {}_\Lambda L_{\mathrm{nc3}} - \frac{1}{16} C_{L\alpha} \rho U_n^2 b_n^4 \tan\Lambda\left[(\delta_r + 1)\frac{\lambda'}{b_n} + \delta_r \frac{\partial \lambda}{\partial \bar{y}}\tan\Lambda\right] \tag{15}$$

$${}_\Lambda M_{\mathrm{nc}}(\bar{y}, \tau) = -\frac{1}{16} \rho C_{L\alpha_n} b_n^2 U_n^2 \alpha'' \tag{16}$$

Herein, the spanwise rates of change of bending and twist, σ and λ, respectively, are defined as $\sigma = \partial h/\partial \bar{y}$ and $\lambda = \partial \alpha/\partial \bar{y}$. In these equations, and in the following ones, the terms affected by the tracer δ_r are generated by the last underlined term in the expression of the downwash velocity [Eq. (11)]. When these terms are discarded, $\delta_r = 0$, and when they are retained, $\delta_r = 1$.

Substituting Eqs. (12) and (13) into Eq. (6) and Eqs. (12), (13), (15), and (16) into Eq. (14) results in the unsteady lift and aerodynamic moment expressed in the time domain. To facilitate the computations, the available approximate expressions for $\phi(\tau)$ and for $C(k)$ (Refs. 11 and 14–18) can be used in the Laplace transformed space. Alternatively, an approximation in terms of exponential polynomials or quasi polynomials can be applied for this case as well. In the case of the supersonic unsteady aerodynamics, the advantage of using such representations was emphasized in Ref. 19. In our numerical simulation, Jones's approximation of Wagner's function was used (see Ref. 11).

The expressions of lift and aerodynamic moment in the time domain, ${}_\Lambda L_a(\bar{y}, \tau)$ and ${}_\Lambda M_a(\bar{y}, \tau)$, can be used to determine the subcritical aeroelastic response of swept wings. However, when the aeroelastic response of wings to time-dependent external excitations is required, the unsteady aerodynamic loads ${}_\Lambda L_a$ and ${}_\Lambda M_a$ have to be supplemented by those corresponding to the involved pulses. This will be considered next, and an illustration of the capabilities provided by this method will be presented.

2. Frequency and Laplace Domains

A number of steps enabling one to express the unsteady lift and moment in the frequency and Laplace domains should be implemented. To this end, the following sequence of operations is applied: 1) replace $s \to ik_n$ in Eqs. (6) and (7) converted to Laplace transformed space, 2) use the relationship between Laplace transform of Wagner and Theodorsen's functions [Eq. (2)], and 3) represent the time dependence of displacement and aerodynamic quantities as

$$\alpha(\bar{y}, \tau) = f_\alpha(\bar{y})\tilde{\alpha}(\tau, k_n) = f_\alpha(\bar{y})\alpha_0 e^{ik_n\tau} \tag{17a}$$

$$h(\bar{y}, \tau) = f_h(\bar{y})\tilde{h}(\tau, k_n) = f_h(\bar{y})h_0 e^{ik_n\tau} \tag{17b}$$

$${}_\Lambda L_a(\bar{y}, k_n, \tau) = {}_\Lambda \bar{L}_a(\bar{y}, k_n)e^{ik_n\tau} \tag{17c}$$

$${}_\Lambda M_\alpha(\bar{y}, k_n, \tau) = {}_\Lambda \bar{M}_\alpha(\bar{y}, k_n)e^{ik_n\tau} \tag{17d}$$

In this analysis $f_\alpha(\bar{y})$ and $f_h(\bar{y})$ are chosen to be the decoupled eigenmodes in plunging and twist of the wing structure and are determined to fulfill the boundary conditions identically. These are expressed as

$$f_h(\bar{y}) = F_h\left(\eta \equiv \frac{\bar{y}}{l}\right) = C_1\left[\frac{\sinh\beta_1 + \sin\beta_1}{\cosh\beta_1 + \cos\beta_1}(\cos\beta_1\eta - \cosh\beta_1\eta) + \sinh\beta_1\eta - \sin\beta_1\eta\right] \tag{18}$$

$$f_\alpha(\bar{y}) = F_\alpha\left(\eta \equiv \frac{\bar{y}}{l}\right) = C_2 \sin\beta_2\eta \tag{19}$$

where, for the first bending and torsion eigenmodes, we have $\beta_1 = 0.5969\pi$ and $\beta_2 = \pi/2$. The constants C_1 and C_2 are chosen to normalize $f_h(\bar{y})$ and $f_\alpha(\bar{y})$, to get the unitary maximum deflection at the wing tip. The uncoupled first bending and torsion mode shapes are needed for the evaluations of the terms in Eqs. (A1–A8) and are displayed in Ref. 20. The use of uncoupled modes in flutter calculations is discussed in detail in Ref. 12, among others, and this methodology will be used here.

B. Modified Unsteady Aerodynamic Derivatives

In this section, a closed-form solution of the modified unsteady aerodynamic coefficients for swept wings, which represent an amended version of those in Refs. 1 and 12, have been derived, and their use in the process of the unified aeroelastic formulation of flutter and aeroelastic response of swept aircraft wings has been addressed.

A careful inspection of equations for lift and moment expressed in the time domain [Eqs. (7) and (8)] suggests the following representation of these quantities:

$${}_\Lambda L_a(\bar{y}, k_n, \tau) = \tfrac{1}{2}\rho U_n^2 2b_n\left[k_n H_1(h'/b_n) + k_n H_2\alpha' + k_n^2 H_3\alpha + k_n^2 H_4(h/b_n) + H_5\alpha'' + H_6(h''/b_n)\right] \tag{20}$$

$${}_\Lambda M_\alpha(\bar{y}, k_n, \tau) = \tfrac{1}{2}\rho U_n^2 2b_n^2\left[k_n A_1(h'/b_n) + k_n A_2\alpha' + k_n^2 A_3\alpha + k_n^2 A_4(h/b_n) + A_5\alpha'' + A_6(h''/b_n)\right] \tag{21}$$

In these equations H_i and A_i denote the dimensionless unsteady aerodynamic coefficients, whereas k_n has been included to render the quantities in brackets nondimensional. In a restricted context, such a mixed form of the lift and moment was used in Refs. 21 and 22. Under the assumption of harmonic time dependence of displacements quantities, the frequency-domain counterpart of Eqs. (20–21), expressed in compact form, becomes

$${}_\Lambda \bar{L}_a(\bar{y}, k_n) = \rho U_n^2 k_n^2 b_n[(h_0/b_n)L_1 + \alpha_0 L_2] \tag{22a}$$

$${}_\Lambda \bar{M}_\alpha(\bar{y}, k_n) = \rho U_n^2 k_n^2 b_n^2[(h_0/b_n)M_1 + \alpha_0 M_2] \tag{22b}$$

where the unsteady aerodynamic complex coefficients L_i and M_i can be expressed in terms of unsteady aerodynamic derivatives as

$$L_1 = i\hat{H}_1 + \hat{H}_4, \qquad L_2 = i\hat{H}_2 + \hat{H}_3 \tag{23a}$$

$$M_1 = i\hat{A}_1 + \hat{A}_4, \qquad M_2 = i\hat{A}_2 + \hat{A}_3 \tag{23b}$$

where, for the sake of convenience, these are written as

$$\hat{H}_1 = H_1, \qquad \hat{H}_2 = H_2 \tag{24a}$$

$$\hat{H}_3 = (H_3 - H_5), \qquad \hat{H}_4 = (H_4 - H_6) \tag{24b}$$

$$\hat{A}_1 = A_1, \qquad \hat{A}_2 = A_2 \tag{24c}$$

$$\hat{A}_3 = (A_3 - A_5), \qquad \hat{A}_4 = (A_4 - A_6) \tag{24d}$$

The closed-form solutions for the unsteady aerodynamic derivatives in the frequency domain for swept wings are obtained from Eqs. (22) and are expressed in terms of Wagner's function $\Phi(ik_n)$. When the real and the imaginary parts of these expressions are separated, the unsteady aerodynamic derivatives are obtained in the form displayed in Appendix A. These include the correction for the aspect ratio, sweep angle, and also the spanwise rates of change of bending and twist, σ and λ. For straight wings, these terms become immaterial.

Equations (20) and (21) are used in two contexts, namely, in the frequency and the Laplace space domains. In the former case, the aerodynamic derivatives H_i and A_i have to be used in accordance with Eqs. (A1–A8). This form of the aerodynamic loads will be used to determine the flutter instability via the solution of a complex eigenvalue problem. In the latter case, Eqs. (20) and (21) are used in conjunction with Eqs. (A1–A8), converted to Laplace space domain using the relationships presented earlier. In this case, the governing equations, including the aerodynamic, blast, and gust loads, are converted to an algebraic system of equations in the Laplace transformed space. This formulation of governing equation enables one to address both the aeroelastic response to blast and gust loads and also the flutter instability.

Notice that the flutter analysis can also be conducted in the Laplace space domain. In this case, classical methods such as U–g or p–k methods can be used.

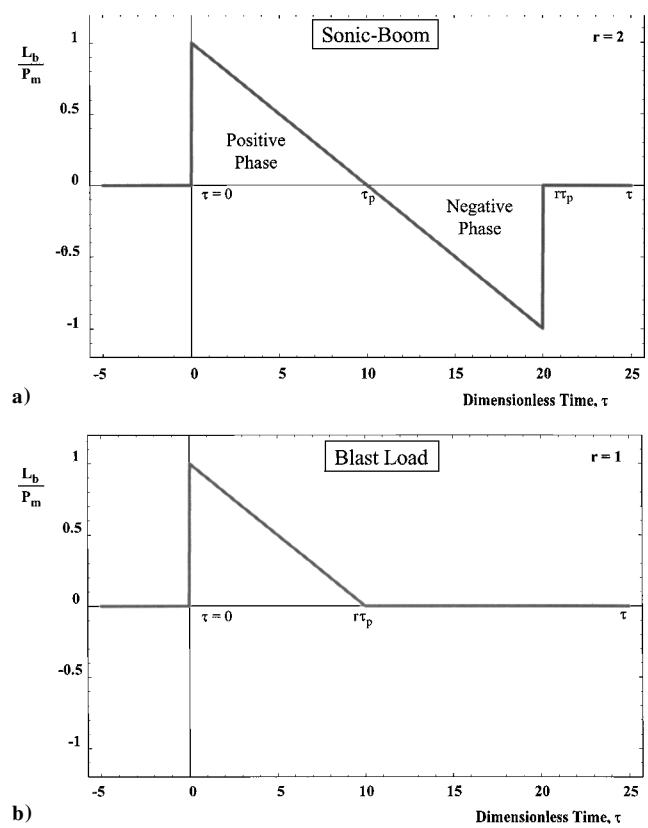

Fig. 3 Pressure pulses for a) sonic boom and b) triangular blast.

C. Aeroelastic Response and Flutter Instability Derived from the Subcritical Aeroelastic Response

An application of the flutter instability and of the aeroelastic response of a swept wing to blast and sonic-boom pressure pulses is considered next. The aeroelastic governing system pertinent to swept wings featuring plunging and twisting degrees of freedom[9,12] and exposed to blast pressure pulses is expressed as

$$EI\frac{\partial^4 w}{\partial \bar{y}^4} + m\frac{\partial^2 w}{\partial t^2} - S_y\frac{\partial^2 \alpha}{\partial t^2} - L_a(\bar{y},t) = L_b(\bar{y},t) \tag{25}$$

$$GJ\frac{\partial^2 \alpha}{\partial \bar{y}^2} + S_y\frac{\partial^2 w}{\partial t^2} - I_y\frac{\partial^2 \alpha}{\partial t^2} - M_a(\bar{y},t) = 0 \tag{26}$$

For the cantilevered wing, the related boundary conditions are

$$\left[w(\bar{y},t) = \frac{\partial w(\bar{y},t)}{\partial \bar{y}} = \alpha(\bar{y},t)\right]\Bigg|_{\bar{y}=0} = 0$$

$$\left[\frac{\partial^2 w(\bar{y},t)}{\partial \bar{y}^2} = \frac{\partial^3 w(\bar{y},t)}{\partial \bar{y}^3} = \frac{\partial \alpha(\bar{y},t)}{\partial \bar{y}}\right]\Bigg|_{\bar{y}=l} = 0 \tag{27}$$

By the use of shape functions, given by Eqs. (18) and (19), the aeroelastic governing equations in dimensionless form become

$$\xi''(\tau) + \bar{\chi}_\alpha \alpha''(\tau) + 2\zeta_h(\bar{\omega}/V_n)\xi'(\tau) + (\bar{\omega}/V_n)^2\xi(\tau) - l_a(\tau) = l_b(\tau) \tag{28}$$

$$\left(\bar{\chi}_\alpha/\bar{r}_\alpha^2\right)\xi''(\tau) + \alpha''(\tau) + (2\zeta_\alpha/V_n)\alpha(\tau) + \alpha(\tau)/V_n^2 - m_\alpha(\tau) = 0 \tag{29}$$

The nondimensional parameters appearing in the preceding equations are displayed in Appendix B.

The sonic-boom and blast overpressures[4,5,23–25] can be expressed as follows:

$$l_b(\tau) = [H(\tau) - H(\tau - r\tau_p)]\wp_m(1 - \tau/\tau_p) \tag{30}$$

where $H(\tau)$ is the Heaviside step function, $\wp_m$ denotes the dimensionless peak reflected pressure in excess of the ambient one (see Refs. 4, 5, and 25 and the references therein), τ_p denotes the positive phase duration of the pulse measured from the time of impact of the structure, and r denotes the shock pulse length factor. A depiction of $l_b/\wp_m$ vs time is displayed in Fig. 3. For $r = 2$ a symmetric N-shaped pulse is obtained (Fig. 3a) and, for $r = 1$, the N-shaped pulse degenerates into a triangular pulse that corresponds to an explosive pulse (Fig. 3b). Equation (30) represents, in a condensed form, the time history of a triangular blast (for which $r = 1, l_b = 0$ for

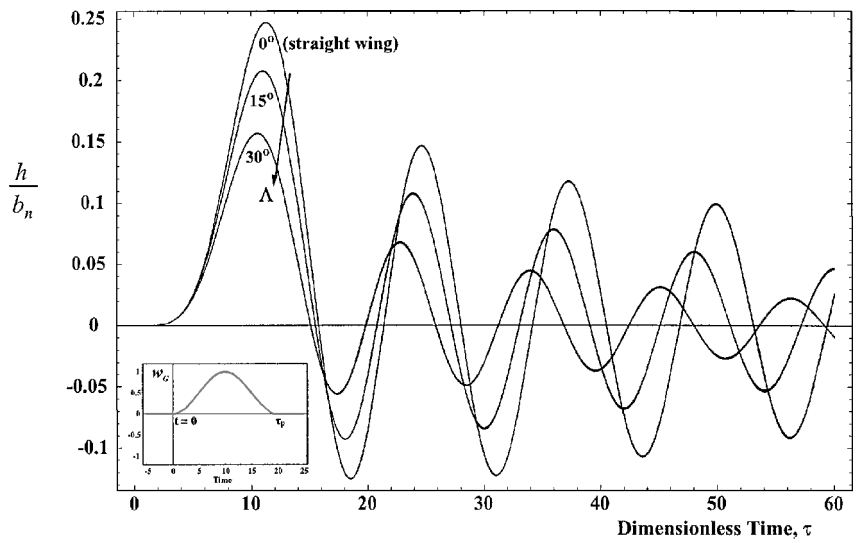

Fig. 4 Predictions of the aeroelastic responses of a straight/swept wing to a gust load, based on exact Theodorsen's function and on its selected approximations supplied in Refs. 13–18; the gust load is expressed in terms of the Küssner's function.

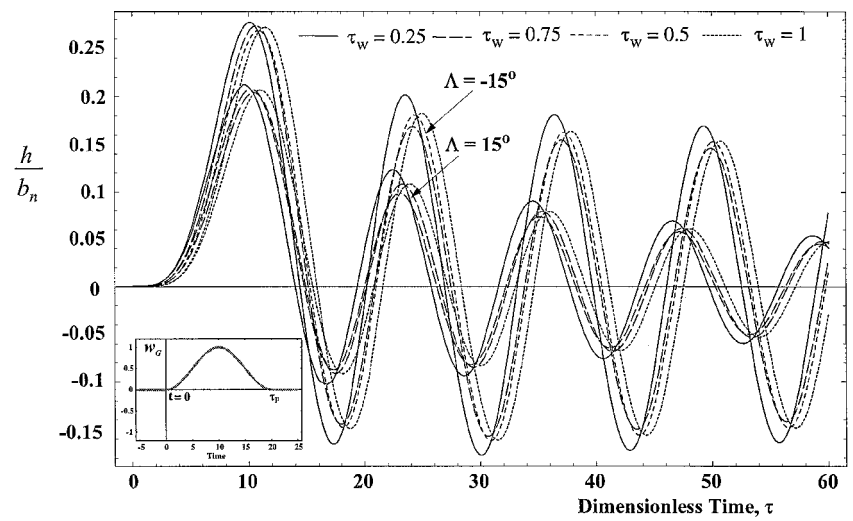

Fig. 5 Predictions of the aeroelastic response time histories of a swept aircraft wings ($\Lambda = \pm 15$ deg) to 1-cosine gust load $[w_G(\tau) = H(\tau)w_0 \sin^2(\pi\tau/\tau_p) - H(\tau - \tau_p)w_0 \sin^2(\pi\tau/\tau_p)]$ for selected values of the propagation speed of the gust τ_w.

$\tau < 0$ and $\tau \geq \tau_p$), whereas, for a sonic boom, when $r \neq 1$, $l_b = 0$ for $\tau < 0$; it simulates the positive and negative phases of the pulse for a $0 < \tau < \tau_p$ and $\tau_p < \tau < r\tau_p$, respectively, and $l_b = 0$ for $\tau \geq r\tau_p$. We assume that the time-dependent pressure pulses reach the peak value in such a short time that the structure can be considered to be loaded instantly and uniformly in the spanwise and chordwise directions.

For this reason, the twist moment in Eq. (26) associated to these pulses is immaterial. Equations (28) and (29) can be converted to the Laplace transformed space and solved for the unknowns, $\hat{\xi}(s) \equiv \mathcal{L}\{\xi(\tau)\}$ and $\hat{\alpha}(s) \equiv \mathcal{L}\{\alpha(\tau)\}$. In addition, in the Laplace space, the unsteady aerodynamic derivatives can be directly obtained from Appendix A by replacing ik_n by s. The same equations, inverted back in the time domain, yield the plunging and pitching time histories and the load factor time history due to the sonic-boom pressure pulse, $\xi(\tau) \equiv \mathcal{L}^{-1}[\hat{\xi}(s)]$ and $\alpha(\tau) \equiv \mathcal{L}^{-1}[\hat{\alpha}(s)]$, respectively.

IV. Results and Discussion

To address the problem of the aeroelastic response by capturing the three-dimensional effects, a modified strip theory will be used.[9] For swept wings, the local lift–curve slope $C_{L\alpha_n}$, involving the corrections of the aspect ratio AR and sweep angle Λ, is obtained from the aerodynamics of swept wings and is expressed as[13,26]

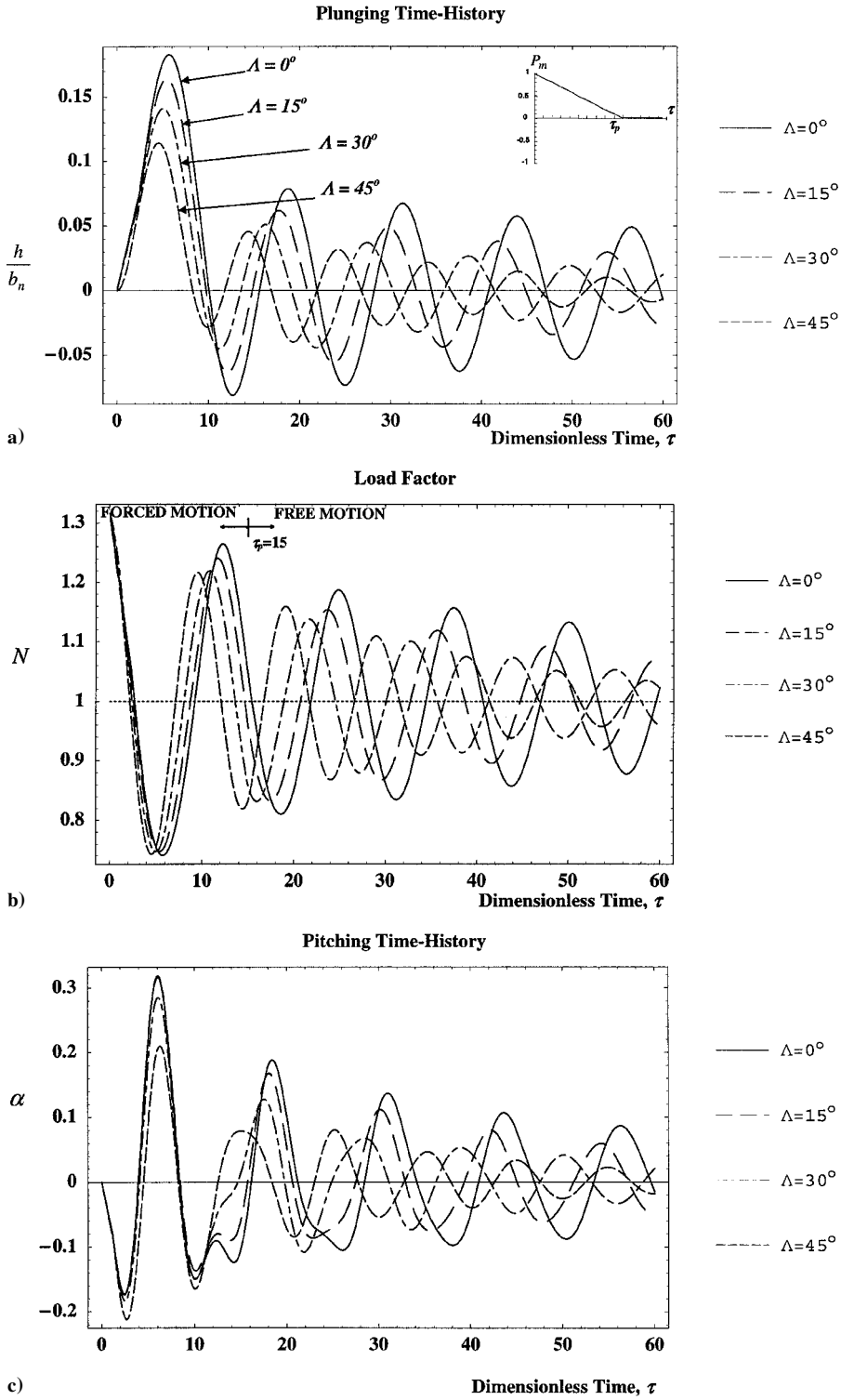

Fig. 6 Influence of angle of sweep Λ on the aeroelastic response to a blast pressure pulse.

$$C_{L\alpha_n} = \frac{C_{L\alpha} AR}{\cos\Lambda C_{L\alpha}/\pi + AR\sqrt{1 + [C_{L\alpha}\cos\Lambda/(\pi AR)]^2}} \quad (31)$$

For moderate-aspect-ratio wings, the maximum influence of the corrective term, identified by the tracer δ_r, is present in the first plunging coefficients $\hat{H}_1$ (see Appendix A). Usually, for all unsteady aerodynamic derivatives, the effect of these terms becomes significant for high sweep angles and for large values of the parameter a_n. In addition, for small-aspect-ratio wings, the effect of the camber becomes significant and as a result should be included. For high-aspect-ratio wings this effect becomes negligibly small.

High-aspect-ratio AR will produce high $\hat{H}_4$, $\hat{A}_1$, and $\hat{A}_4$, and because these are correlated to the plunging displacement, large aerodynamic loads will be induced.

Notice that, for $k \to \infty$, the circulatory components of Theodorsen's function assume the values $F(k) \to \frac{1}{2}$ and $G(k) \to 0$, and the corresponding unsteady aerodynamic derivatives can be determined in agreement with the steady-state solution for lift and aerodynamic moment. In these developments, all of the terms, including the aerodynamic ones associated with $\ddot{h}$ and $\ddot{\alpha}$, have been retained. Usually, these terms are neglected; however, due to the presence of high-frequency components in the blast pressure terms, their effect can be significant.

As a result, the coefficients H_5, H_6 and A_5, A_6 are also maintained. Whereas the aerodynamic coefficients $\hat{H}_1$ and $\hat{A}_2$ are the principal uncoupled aerodynamic damping coefficients in plunging and torsion, respectively, $\hat{H}_2$ and $\hat{A}_1$ are the coupled damping coefficients. As concerns the depiction of $\hat{H}_i$ and $\hat{A}_i$ vs $2\pi/k$, this representation enables one to get an idea of the variation of these quantities with that of the normal freestream speed U_n.

A. Subcritical Aeroelastic Response

The graphs depicting the aeroelastic response time history to gust and blast pulses are displayed in Figs. 4–13. In each of these graphs the corresponding type of pressure load is indicated in an inset.

In addition, the parameters in use for the simulations, unless otherwise specified, are chosen as $V_n = 1$, $\mu = 10$, $\bar{\omega} = 0.5$, $r_\alpha = 0.5$, $\chi_\alpha = 0.125$, $\zeta_\eta = \zeta_\alpha = 0$, $a_n = -0.2$, $\wp_m = 1$, $w_0 = 1$, $\tau_p = 15$, and $r = 1$ or 2. Although the numerical simulations concern the aeroelastic responses at the wing tip cross section, $\eta = 1$, the time history of displacement variables can be evaluated in any cross section of the aircraft wing.

1. *Response to 1-Cosine Gust Load*

For obvious reasons (see, for example, Ref. 1), the time-dependent gust loads have a character different from that of the blast loads. For both traveling sharp-edged or stationary gusts the associated loads involve the use of indicial lift and moment functions. With regards to this similarity, a parameter that identifies the propagation speed of the gust, $\tau_w = V_n/(V_n + V_g)$, is used (see, for example, Refs. 8 and 27). On the other hand, because a twist moment is also induced by the gust, this load involves both equations of motion.

In Fig. 4, predictions of the aeroelastic response of a straight/swept wing to a gust load (evaluated via gust penetration Küssner's function and indicated in the inset of Fig. 4) are presented. For their computation, both the exact and selected approximate expressions of Theodorsen's function (see Refs. 14–18) have been used. The differences in the response occurring as a result of these approximations are indiscernible, indicative of the high accuracy of the approximations involving the expression of $C(s)$.

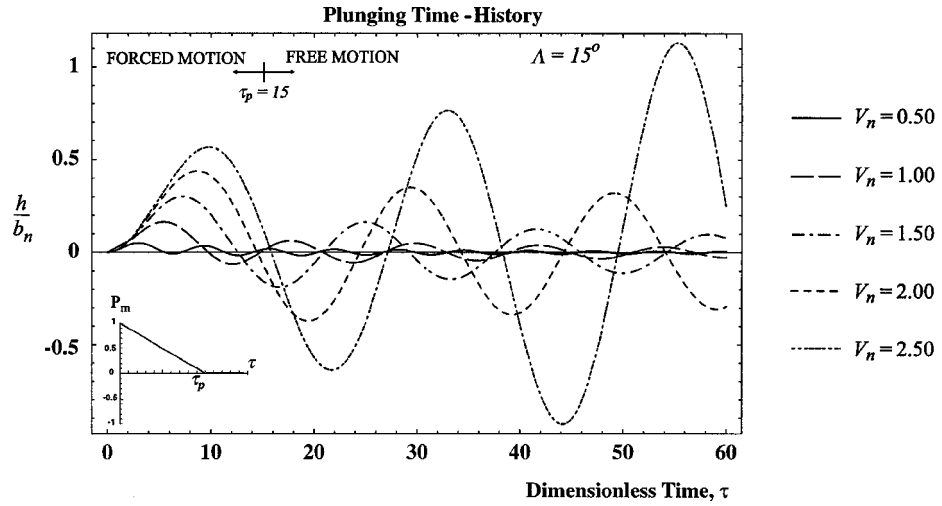

Fig. 7 Influence of the speed parameter V_n on the response of a swept aircraft wing ($\Lambda = 15$ deg) to blast pulses.

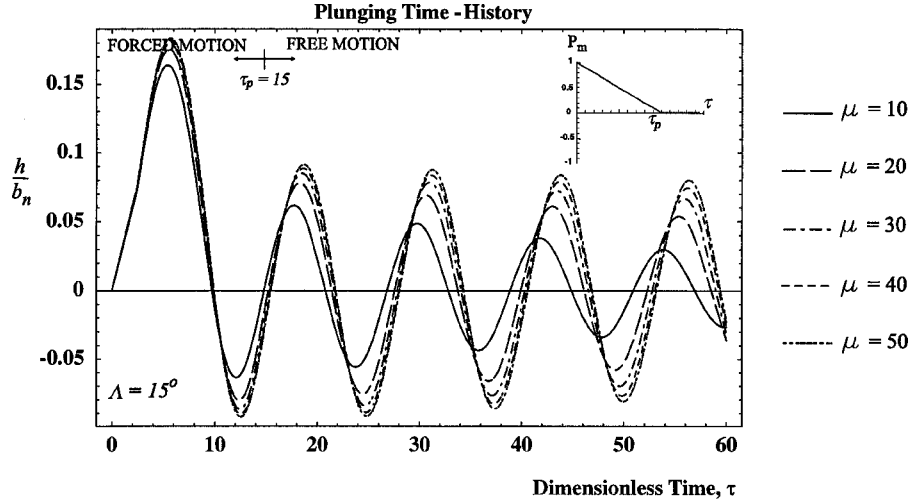

Fig. 8 Influence of the mass parameter μ on the response of a swept aircraft wing ($\Lambda = 15$ deg) to blast pulses.

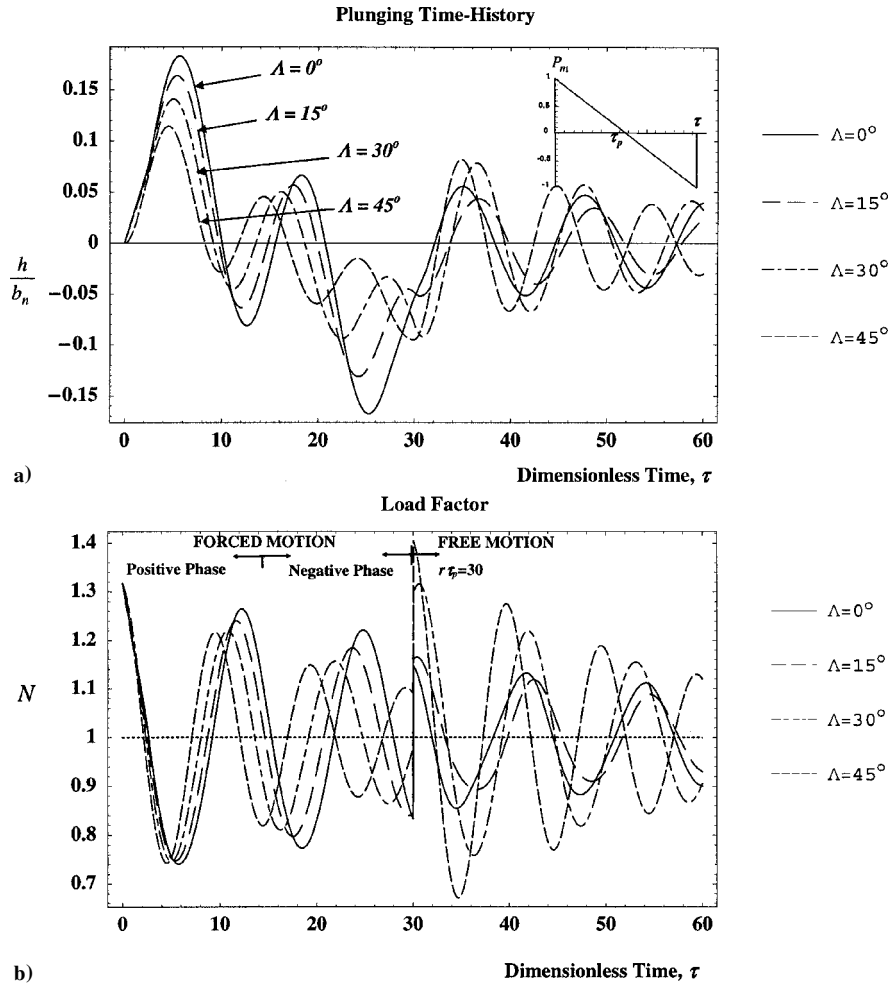

Fig. 9 Influence of the sweep angle Λ on the response of a wing to sonic-boom pulses.

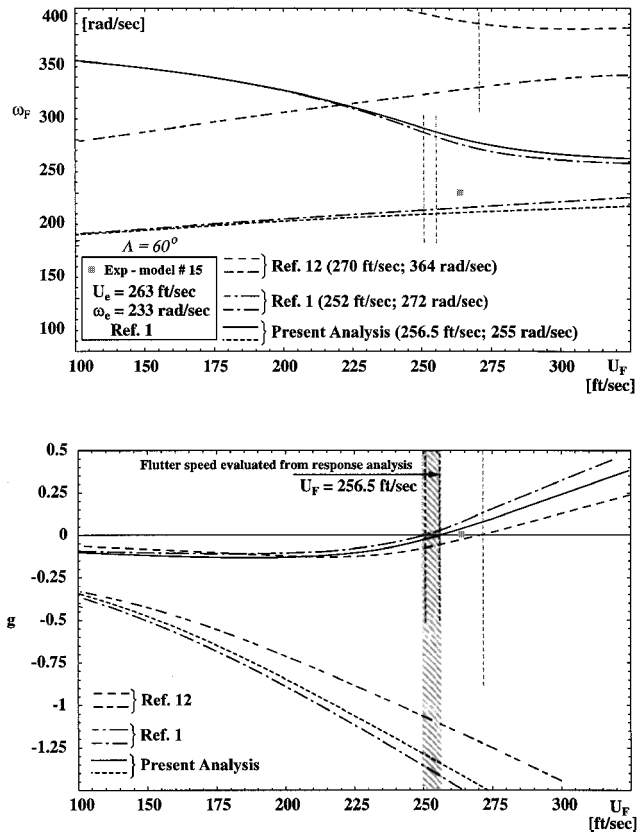

Fig. 10 Flutter calculation via *U–g* method.[1]

For a ±15-deg swept wing encountering a traveling gust, Fig. 5 highlights the influence on the plunging time history of the propagation speed of the gust for the cases of $\tau_w = 1.00$ (corresponding to the Küssner's function) and $\tau_w = 0.25, 0.50$, and 0.75, that is, for selected intermediate values of the gust speed. A full discussion of the implication of the propagation speed of the gust are beyond the scope of this paper. Note that, even if the aerodynamic loads are affected by the traveling gust,[8,27] the maximum amplitudes of the response shift toward smaller times and are only slightly affected by the propagation speed of the gust. The results reveal that, in the case of a swept-back wing, the amplitudes of the plunging displacement are lower than those of its swept-forward wing counterpart.

2. *Response to Blast and Sonic-Boom Pressure Signatures*

The graphs in Figs. 6 supply the dimensionless plunging ($\xi \equiv h/b_n$) and pitching (α) displacements and the load factor ($N \equiv 1 + h''/g$, where g is the acceleration of gravity) time history aeroelastic responses to a blast pressure pulse. It becomes apparent that an increase of the wing sweep angle results in a decrease of the severity of the pulse signature.

In addition, the plunging–pitching coupling helps to reduce the amplitude of the aeroelastic response.[20] The load factor N has its maximum at $\tau = 0$, when the first impulse due to the blast load occurs.

Figure 7 highlights the effect of the speed parameter

$$V_n (\equiv U_n / b_n \omega_\alpha)$$

on plunging time history of the swept aircraft wing ($\Lambda = 15$ deg) subjected to blast pulses. It becomes apparent that the amplitude of the response time history increases with the increase of V_n. In a fixed speed range, the amplitude decays due to the involved subcritical response. However, for $V_n \cong 2.12$, the flutter instability is impending.

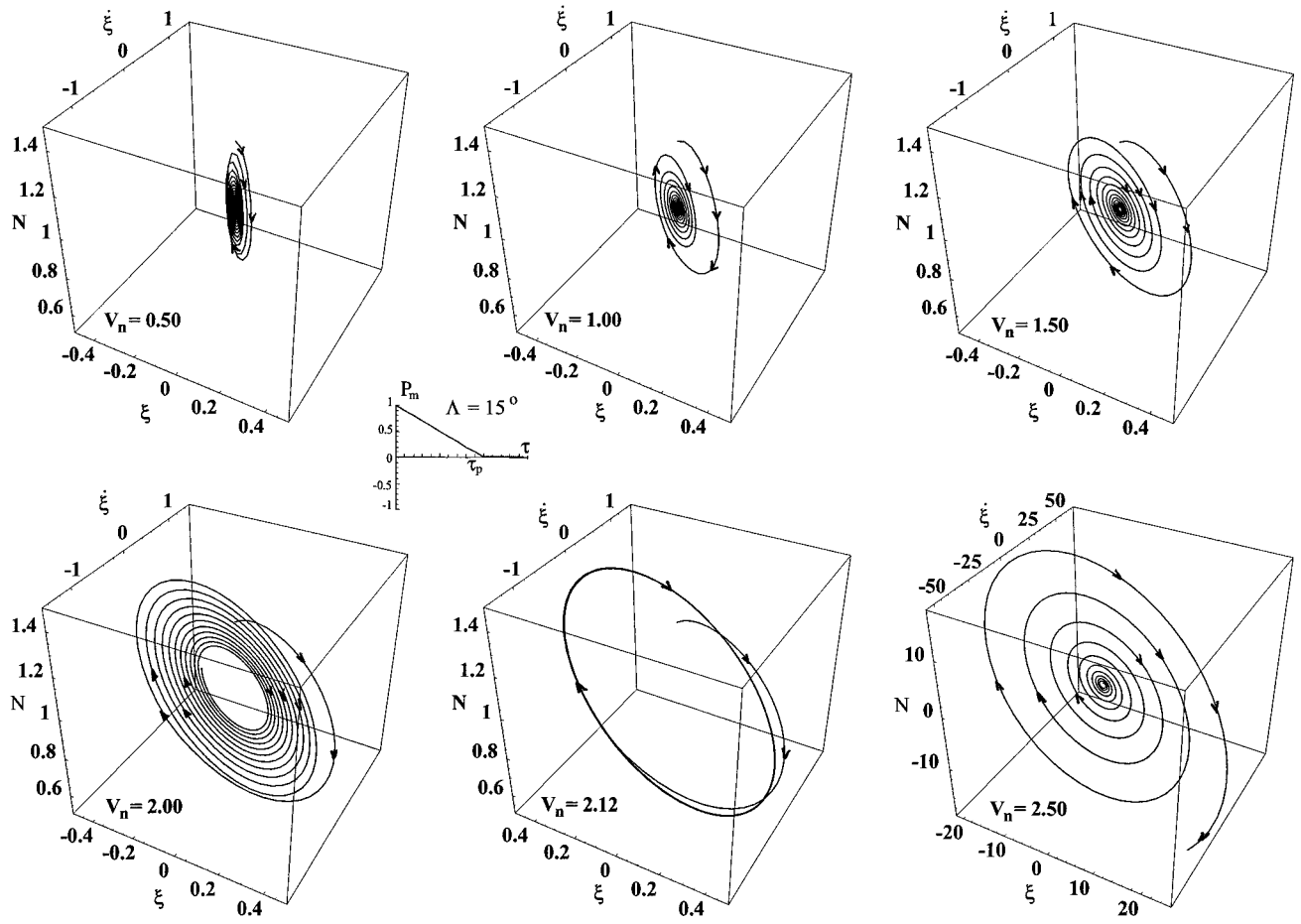

Fig. 11 Three-dimensional phase-space portrait depicting the dimensionless plunging deflection time history of swept aircraft wing ($\Lambda = 15$ deg) to blast pressure signature vs the load factor N for selected values of the speed parameter.

The effect of the mass parameter $\mu(\equiv m/\pi\rho b_n^2)$, for a swept wing characterized by $\Lambda = 15$ deg, is indicated in Fig. 8. The increase in the mass ratio results in the increase of the plunging and pitching displacement amplitudes. Therefore, for higher mass ratios and AR, the motion damps out at larger times. Note that the response to sonic-boom pressure pulses involves two different regimes (Figs. 9a and 9b): one for which $0 < \tau < 30$ corresponds to the forced motion and the other for which $\tau > 30$ corresponds to free motion. The jump in the time history of N (Fig. 9b) is due to the discontinuity in the load occurring at $\tau = 30$. For explosive pressure pulses, where $r = 1$, this jump does not occur (Fig. 6b). Moreover, when the sweep angle is increased, the effect of the blast becomes less severe.

B. Flutter Instability Boundary

The unsteady aerodynamic derivatives, expressed in the Laplace transformed space, are applied in the flutter analysis, and the results are displayed in Fig. 10. To validate our approach, a comparison of the flutter prediction via indicial function of a cantilever metallic swept wing of $AR = 4$ and $\Lambda = 60$ deg is presented. The results reveal that the predictions provided by the present approach (i.e., $U_F = 256.5$ ft/s and $\omega_F = 255$ rad/s) even in the case of such a low aspect ratio and large sweep angle wing are in excellent agreement with those displayed in Ref. 1 (experimental model 15). On the same graph, comparisons of the results based on the assumptions of Refs. 1 and 12 with those based on the present analysis are presented. Whereas, in our approach, the camber effect and the corrections related to the aspect ratio and sweep angle were included, in Ref. 12 these effects are not addressed at all. In Ref. 1 these effects are partially considered. The critical value of the flutter speed is obtained herein via the solution of both the complex eigenvalue problem and from the response analysis. In Fig. 10 the range in which the flutter instability occurs is determined from the response time histories. The flutter predictions based on both methods show an excellent agreement. In addition, to further validate this approach, the flutter speed of Goland's[28] and Goland and Luke's[29] cantilevered wing ($AR = 6.67$), which constitutes a standard of comparison throughout the specialized literature, has been evaluated via the present approach from the response to blast loads. The flutter characteristics provided by the present approach (490 km/h and 69.12 rad/s), are in excellent agreement with Goland's[28] and Goland and Luke's[29] exact results (494.1 km/h and 70.69 rad/s) and with Ref. 30 (495 km/h and 70.37 rad/s), in which an exact solution methodology was used. There is also an improvement of the flutter prediction when compared with the results provided by Patil et al.[31] (488.3 km/h and 70.2 rad/s) and with the ones derived by finite element codes COMBOF[32] (483.1 km/h and 70.81 rad/s), SADSAM[33] (472.5 km/h, –), and state vector[34] (486 km/h, –), where the dashes indicate that the value of the flutter frequency was not reported.

An original point prompted in this paper concerns the fact that the evolution of the aeroelastic system can be graphically illustrated by examining its motion in the phase space, rather than in the real space and by recognizing that the trajectory depicted in this space represents the complete time history of the system (see Figs. 11–13). The trajectory of motion describes an orbit with constant amplitude (the center), which corresponds to the flutter conditions that coincide with those obtained from the eigenvalue analysis. For $V < V_F$, as time unfolds, a decay of the amplitude is experienced, which reflects that, in this case, a subcritical response is involved (stable focal point), whereas, for $V > V_F$, the response becomes unbounded, implying that the occurrence of the flutter instability is impending (unstable focal point).

Figure 11 highlights a three-dimensional phase-space portrait (ξ vs $\dot{\xi}$ and N) of the plunging time-history response to blast load of a swept aircraft wing ($\Lambda = 15$ deg) for selected values of the speed

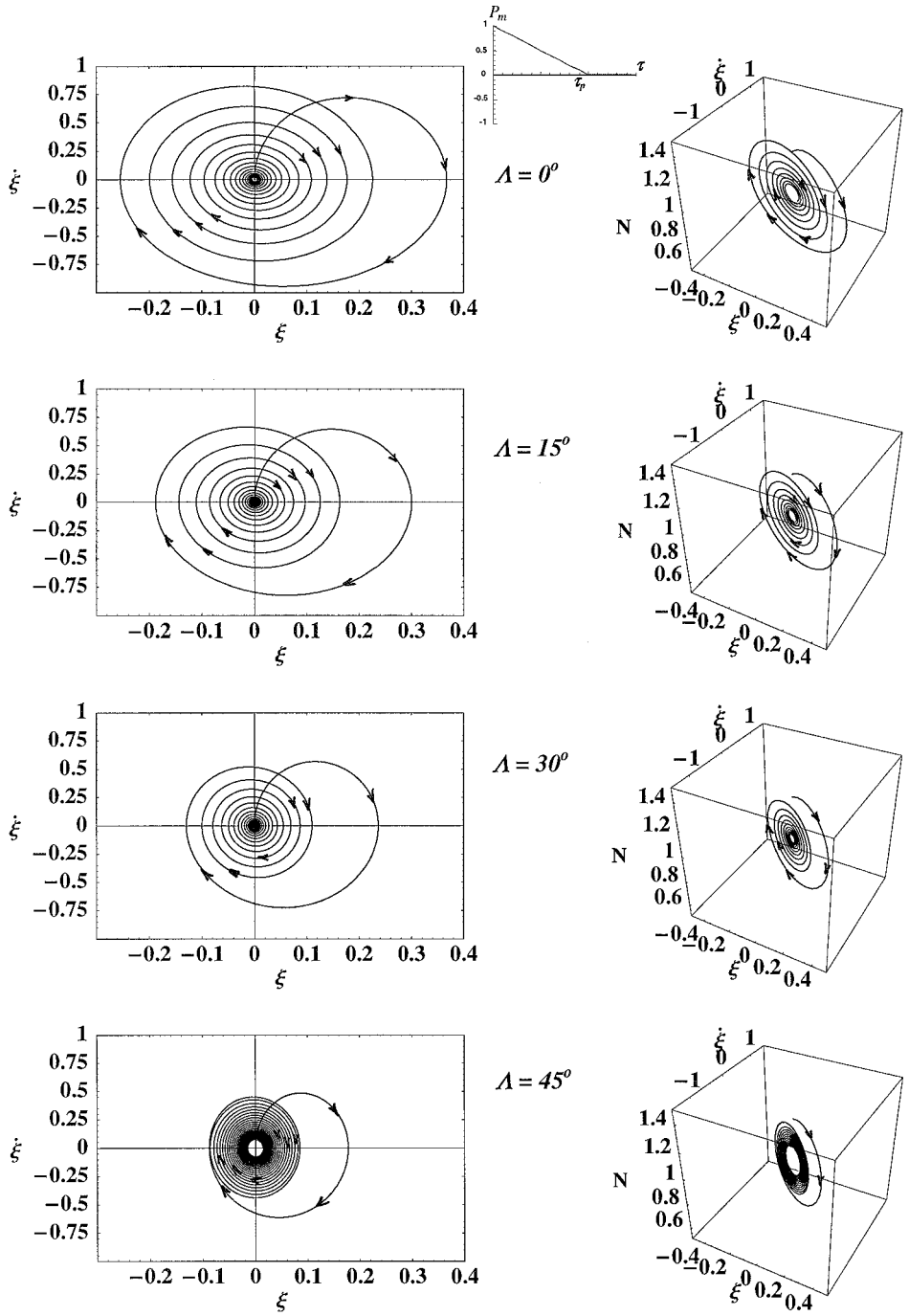

Fig. 12 Phase-plane ($\xi, \dot{\xi}$) and phase-space portraits ($\xi, \dot{\xi}, N$) depicting the dimensionless plunging deflection time history of a swept aircraft wing to blast pressure signature, for selected values of the sweep angle.

parameter. For $V_n \cong 2.12$, representing the critical speed at which the periodic solution has been obtained, the occurrence of the flutter instability is impending.

Figure 12 shows the phase-plane portrait and the relative three-dimensional plots (vs the load factor N) for selected values of the sweep angle Λ. With the increase of the sweep angle, the motion damps out at smaller times, and a decay of the amplitude of the response as well as of the load factor is experienced.

Figure 13 supplies three-dimensional pictorial views of the plunging and pitching motions in the proximity of the flutter boundary vs the variation of the sweep angle. These plots provide a clear view of the evolution of the maxima of displacement amplitudes.

Note that the methodology presented here can be extended to the compressible flight speed regimes. For that case, appropriate indicial functions for the compressible subsonic, supersonic, and hypersonic flight speed regimes have to be used.

In Refs. 35–40, the concept of indicial functions in subsonic compressible flow has been developed, and an approximation and validation of indicial functions for any value of Mach number in the compressible speed range was obtained. In contrast to the incompressible case, the indicial functions in subsonic compressible flow are not analytic, except for limited instants of time. Following the formulation in Refs. 35–37, a new set of indicial functions, for the plunging and pitching degrees of freedom, can be adopted and implemented. Moreover, an advanced structural model of aircraft wings, as considered, for example, in Ref. 30, can be adopted for such a study. However, the goal of the paper was not to illustrate the implications of nonclassical structural features, but only to develope some basic principles that can further be extended

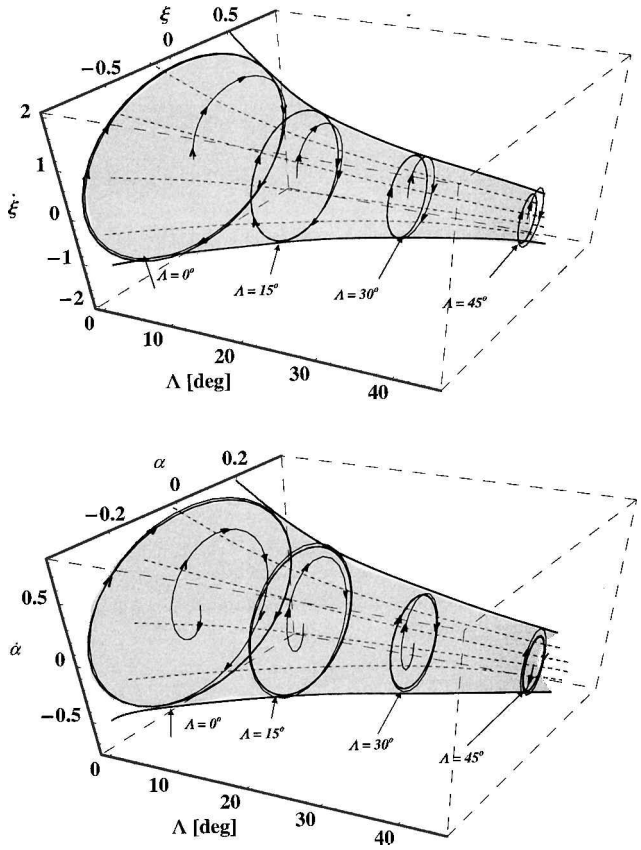

Fig. 13 Cone of stability orbits depicting the envelope of the upper bound values of the dimensionless plunging and pitching deflection time histories of an aircraft wing vs Λ to blast pressure signatures.

and properly exploited to more complex structural wing configurations.

V. Conclusions

A unified treatment of swept lifting surfaces in time and frequency domains has been presented, and the usefulness, in this context, of the aerodynamic indicial function concept was emphasized. The time-domain representation is essential toward determination of the dynamic aeroelastic response to time-dependent external loads. Two ways of representing the aeroelastic response have been used, namely, the classical one, consisting of displaying the time histories of plunging, pitching, and load factor, and the phase-space representation that provides useful information about the behavior of the aeroelastic system.

Applications assessing the versatility of the methodology presented here toward the approach of both the subcritical aeroelastic response and flutter instability of three-dimensional swept aircraft wings have been presented. The concept of the stability boundary and its enhancement via the use of the variable sweep wing geometry have been illustrated. The unified formulation presented in this work can be extended to various flight speed regimes. The method may have applications toward determination of the critical flutter speed via the experimental investigation of the aeroelastic response of aircraft wings to pulse loadings. Moreover, it creates the theoretical basis for a unified nonlinear aeroelastic approach of swept aircraft wings based on the use of nonlinear indicial functions.

Appendix A: Unsteady Aerodynamic Derivatives

$$\hat{H}_1 = -C_{L\alpha_n}\left\{\frac{F(k_n)}{k_n} f_h + \left[\frac{G(k_n)}{k_n} + \frac{1}{2}(1+\delta_r)\right]\frac{1}{k_n}\frac{\partial f_h}{\partial \eta}\frac{\sin\Lambda}{2AR}\right\} \tag{A1}$$

$$\hat{H}_2 = -\frac{C_{L\alpha_n}}{k_n}\left\{\left[\left(\frac{1}{2}-a_n\right)F(k_n) + \frac{G(k_n)}{k_n} + \frac{1}{2}\right] f_\alpha + \left[\frac{2G(k_n)}{k_n}\left(\frac{1}{2}-a_n\right) - \frac{1}{2}a_n(1+\delta_r)\right]\frac{\partial f_\alpha}{\partial \eta}\frac{\sin\Lambda}{2AR}\right\} \tag{A2}$$

$$\hat{H}_3 = -C_{L\alpha_n}\left\{\left[\frac{F(k_n)}{k_n^2} - \frac{G(k_n)}{k_n}\left(\frac{1}{2}-a_n\right) + \frac{1}{2}a_n\right] f_\alpha + \left[F(k_n)\left(\frac{1}{2}-a_n\right) + \frac{1}{2}\delta_r\right]\frac{1}{k_n^2}\frac{\partial f_\alpha}{\partial \eta}\frac{\sin\Lambda}{2AR} - \delta_r\frac{1}{2}\frac{1}{k_n^2}\frac{\partial^2 f_\alpha}{\partial \eta^2}a_n\left(\frac{\sin\Lambda}{2AR}\right)^2\right\} \tag{A3}$$

$$\hat{H}_4 = C_{L\alpha_n}\left\{\left[\frac{1}{2} + \frac{G(k_n)}{k_n}\right] f_h - \left[F(k_n)\frac{\partial f_h}{\partial \eta} + \delta_r\frac{1}{2}\frac{\partial^2 f_h}{\partial \eta^2}\frac{\sin\Lambda\cos\Lambda}{AR}\right]\frac{1}{k_n^2}\frac{\sin\Lambda}{2AR}\right\} \tag{A4}$$

$$\hat{A}_1 = \frac{C_{L\alpha_n}}{k_n}\left\{\left(\frac{1}{2}+a_n\right)F(k_n) f_h + \left[\left(\frac{1}{2}+a_n\right)\frac{G(k_n)}{k_n} + \frac{1}{2}a_n(\delta_r+1)\right]\frac{\partial f_h}{\partial \eta}\frac{\sin\Lambda}{2AR}\right\} \tag{A5}$$

$$\hat{A}_2 = \frac{C_{L\alpha_n}}{2k_n}\left\{\left[\left(a_n-\frac{1}{2}\right) + \left(\frac{1}{2}+a_n\right)\frac{2G(k_n)}{k_n} - \left(a_n^2-\frac{1}{4}\right)2F(k_n)\right] f_\alpha + \left[\left(\frac{1}{4}-a_n^2\right)\frac{2G(k_n)}{k_n} - (\delta_r+1)\left(\frac{1}{8}+a_n^2\right)\right]\frac{\partial f_\alpha}{\partial \eta}\frac{\sin\Lambda}{2AR}\right\} \tag{A6}$$

$$\hat{A}_3 = \frac{C_{L\alpha_n}}{4k_n^2}\left\{\left[(1+2a_n)2F(k_n) + (4a^2-1)G(k_n)k_n + \left(2a_n^2+\frac{1}{4}\right)k_n^2\right] f_\alpha + \left[\left(1-4a_n^2\right)F(k_n) - (1-\delta_r 2a_n)\right] \times \frac{\partial f_\alpha}{\partial \eta}\frac{\sin\Lambda}{2AR} - \delta_r\left(\frac{1}{4}+2a_n^2\right)\frac{\partial^2 f_\alpha}{\partial \eta^2}\left(\frac{\sin\Lambda}{2AR}\right)^2\right\} \tag{A7}$$

$$\hat{A}_4 = -C_{L\alpha_n}\left\{\left[\frac{1}{2}a_n + \left(\frac{1}{2}+a_n\right)\frac{G(k_n)}{k_n}\right] f_h - \left[\left(\frac{1}{2}+a_n\right)F(k_n)\frac{\partial f_h}{\partial \eta} + \delta_r\frac{1}{2}a_n\frac{\partial^2 f_h}{\partial \eta^2}\frac{\sin\Lambda}{2AR}\right]\frac{1}{k_n^2}\frac{\sin\Lambda}{2AR}\right\} \tag{A8}$$

Here the aspect ratio AR and the spanwise dimensionless coordinate η are defined as $AR = l_n/b_n\cos^2\Lambda$ and $\eta = \bar{y}/l$, respectively. For $\Lambda = 0$, the expressions of aerodynamic coefficients reduce to those pertinent to straight wings.

Appendix B: Nondimensional Parameters for Flutter and Response Analyses

$$l_a = \frac{L_a b_n}{m U_n^2\left(\int_0^1 f_h^2\,\mathrm{d}\eta\right)}, \qquad m_a = \frac{M_\alpha b_n^2}{I_y U_n^2\int_0^1 f_\alpha^2\,\mathrm{d}\eta}$$

$$V_n = \frac{U_n}{b_n \omega_\alpha}, \qquad \wp_m = \frac{P_m b_n}{m U_n^2 \left(\int_0^1 f_h^2 \, \mathrm{d}\eta \right)}, \qquad \mu = \frac{m}{C_{L\alpha} \rho b_n^2}$$

$$\zeta_h = \frac{c_h}{2m\omega_h}, \qquad \xi = \frac{h}{b_n}, \qquad \zeta_\alpha = \frac{c_\alpha}{2I_\alpha \omega_\alpha}, \qquad \bar{\omega} = \frac{\omega_h}{\omega_\alpha}$$

$$\bar{r}_\alpha^2 = \frac{I_y}{m b_n^2} \left(\frac{\int_0^1 f_\alpha^2 \, \mathrm{d}\eta}{\int_0^1 f_h^2 \, \mathrm{d}\eta} \right), \qquad \bar{\chi}_\alpha = \frac{S_\alpha}{mb} \left(\frac{\int_0^1 f_\alpha f_h \, \mathrm{d}\eta}{\int_0^1 f_h^2 \, \mathrm{d}\eta} \right)$$

Acknowledgment

The work reported here was partially supported by the NASA Langley Research Center through Grant NAG-1-2281.

References

[1]Bisplinghoff, R. L., Ashley, H., and Halfman R. L., *Aeroelasticity*, Dover, New York, 1996, pp. 281–293, 332–353.

[2]Lomax, H., "Indicial Aerodynamics," *AGARD Manual on Aeroelasticity*, edited by R. Mazet, London, 1960, pp. 1–58.

[3]Tobak, M., "On the Use of the Indicial Function Concept in the Analysis of Unsteady Motion of Wings and Wing–Tail Combinations," NACA R-1188, Jan. 1954.

[4]Librescu, L., and Nosier, A., "Response of Laminated Composite Flat Panels to Sonic-Boom and Explosive Blast Loading," *AIAA Journal*, Vol. 28, No. 2, 1990, pp. 345–352.

[5]Librescu, L., and Na, S. S., "Dynamic Response of Cantilevered Thin-Walled Beams to Blast and Sonic-Boom Loadings," *Journal of Shock and Vibration*, Vol. 5, No. 1, 1998, pp. 23–33.

[6]Karpel, L., "Design for Active Flutter Suppression and Gust Alleviation Using State-Space Aeroelastic Modeling," *Journal of Aircraft*, Vol. 19, No. 3, 1982, pp. 221–227.

[7]Roger, K. L., "Airplane Math Modeling Methods for Active Control Design," CP-228, AGARD, Aug. 1977.

[8]Drischler, J. A., and Diederich, F. W., "Lift and Moment Responses to Penetration of Sharp-Edged Traveling Gusts, with Application to Penetration of Weak Blast Waves," NACA TN-3956, May 1957.

[9]Yates, C., "Calculation of Flutter Characteristics for Finite-Span Swept or Unswept Wings at Subsonic and Supersonic Speeds by a Modified Strip Analysis," NACA RM-L57L10, May 1958.

[10]Edwards, J.W., Ashley, H., and Breakwell, J.V., "Unsteady Aerodynamic Modeling for Arbitrary Motions," *AIAA Journal*, Vol. 17, No. 4, 1979, pp. 365–374.

[11]Fung, Y. C., *An introduction to the Theory of Aeroelasticity*, Wiley, New York, 1955, pp. 206–216.

[12]Barmby, J. G., Cunningham, H. J., and Garrick, I. E., "Study of Effects of Sweep on the Flutter of Cantilever Wings," NACA R-1014, 1951.

[13]Flax, A. H., "Aeroelasticity and Flutter, in High Speed Problems of Aircraft and Experimental Methods," *High Speed Aerodynamics and Jet Propulsion*, Vol. 8, edited by H. F. Donovan and H. R. Lawrence, Princeton Univ. Press, Princeton, NJ, 1961, pp. 161–417.

[14]Peterson, L. D., and Crawley, E. F., "Improved Exponential Time Series Approximations of Unsteady Aerodynamic Operators," *Journal of Aircraft*, Vol. 25, No. 2, 1988, pp. 121–127.

[15]Eversman, W., and Tewari, A., "Modified Exponential Series Approximation for the Theodorsen Function," *Journal of Aircraft*, Vol. 28, No. 9, 1991, pp. 553–557.

[16]Dowell, E. H., "A Simple Method for Converting Frequency Domain Aerodynamics to the Time Domain," NASA TM-81844, 1980.

[17]Venkatesan, C., and Friedmann, P. P., "New Approach to Finite-State Modeling of Unsteady Aerodynamics," *AIAA Journal*, Vol. 24, No. 12, 1986, pp. 1889–1897.

[18]Leishman, J. G., and Nguyen, K. Q., "State-Space Representation of Unsteady Airfoil Behavior," *AIAA Journal*, Vol. 28, No. 5, 1990, pp. 836–844.

[19]Librescu, L., "Unsteady Aerodynamic Theory of Lifting Surfaces and Thin Elastic Bodies Undergoing Arbitrary Small Motions in a Supersonic Flow Field," *Quarterly Journal of Mechanics and Applied Mathematics*, Vol. 40, Pt. 4, 1987, pp. 539–557.

[20]Marzocca, P., Librescu, L., and Silva, W. A., "Aerodynamic Indicial Functions and Their Use in Aeroelastic Formulation of Lifting Surfaces," AIAA Paper 2000-0000, 2000.

[21]Simiu, E., and Scanlan, R. H., "Aeroelastic Phenomena," *Wind Effects on Structures, An Introduction to Wind Engineering*, 2nd ed., Wiley, New York, 1986, pp. 228–231.

[22]Scanlan, R. H., "Aeroelastic Problems of Civil Engineering Structures," *A Modern Course in Aeroelasticity*, edited by E. H. Dowell, 3rd rev. and enlarged ed., Kluwer Academic, Norwell, MA, 1996, pp. 327–335.

[23]Pilon, A., and Lyrintzis, A. S., "Data-Parallel Total Variation Diminishing Method for Sonic Boom Calculations," *Journal of Aircraft*, Vol. 33, No. 1, 1996, pp. 87–92.

[24]Gottlieb, J. J., and Ritzel, D. V., "Analytical Study of Sonic Boom from Supersonic Projectiles," *Progress in Aerospace Sciences*, Vol. 25, 1988, pp. 131–188.

[25]Department of the Army, "Fundamentals of Protective Design for Conventional Weapons," TM 5-855-1, Nov. 1986.

[26]Bisplinghoff, R. L., and Ashley, H., *Principles of Aeroelasticity*, Dover, New York, 1975, pp. 91–103.

[27]Leishman, J. G., "Unsteady Aerodynamics of Airfoils Encountering Traveling Gusts and Vortices," *Journal of Aircraft*, Vol. 34, No. 6, 1997, pp. 719–729.

[28]Goland, M., "The Flutter of a Uniform Cantilever Wing," *Journal of Applied Mechanics*, Vol. 12, No. 4, 1945, pp. A-198–A-208.

[29]Goland, M., and Luke, Y. L., "The Flutter of a Uniform Wing with Tip Weights," *Journal of Applied Mechanics*, Vol. 15, No. 1, 1948, pp. 13–20.

[30]Karpouzian, G., and Librescu, L., "Nonclassical Effects on Divergence and Flutter of Anisotropic Swept Aircraft Wings," *AIAA Journal*, Vol. 34, No. 4, 1996, pp. 786–794.

[31]Patil, M. J., Hodges, D. H., and Cesnik, C. E. S., "Nonlinear Aeroelastic Analysis of Complete Aircraft in Subsonic Flow," *Journal of Aircraft*, Vol. 37, No. 5, 2000, pp. 753–760.

[32]Housner, J. M., and Stein, M., "Flutter Analyses of Swept-Wing Subsonic Aircraft with Parameter Studies of Composite Wings," NASA TND-7539, Sept. 1974.

[33]Peterson, L., "SADSAM User's Manual," MSR-10, MacNeal–Schwendler Corp., Dec. 1970.

[34]Lehman, L. L., "Hybrid State Vector Approach to Aeroelastic Analysis," *AIAA Journal*, Vol. 20, No. 10, 1982, pp. 1442–1449.

[35]Leishman, J. G., "Validation of Approximate Indicial Aerodynamic Functions for Two-Dimensional Subsonic Flow," *Journal of Aircraft*, Vol. 25, No. 10, 1988, pp. 914–922.

[36]Leishman, J. G., "Indicial Approximation for Two-Dimensional Subsonic Flow as Obtained from Oscillatory Measurements," *Journal of Aircraft*, Vol. 30, No. 3, 1993, pp. 340–351.

[37]Leishman, J. G., *Principles of Helicopter Aerodynamics*, Cambridge Aerospace Series, Vol. 12, Cambridge Univ. Press, Cambridge, England, U.K., 2000, pp. 302–377.

[38]Mazelsky, B., "Numerical Determination of Indicial Lift of a Two-Dimensional Sinking Airfoil at Subsonic Mach Numbers from Oscillatory Lift Coefficients with Calculations for Mach Number 0.7," NACA TN-2562, Dec. 1951; also NACA TN-2613, Feb. 1952.

[39]Lomax, H., Heaslet, M. A., and Sluder, L., "The Indicial Lift and Pitching Moment for a Sinking or Pitching Two-Dimensional Wing Flying at Subsonic or Supersonic Speeds," NACA TN-2403, July 1951.

[40]Beddoes, T. S., "Practical Computation of the Unsteady Lift," *Vertica*, Vol. 8, No. 1, 1984, pp. 55–71.

E. Livne
Associate Editor